Study on the Thermodynamic Interactions between Isotactic Polypropylene and Ethylene−1-Hexene Random Copolymers by SANS

Motohiro Seki, Hisao Uchida, Youichi Maeda, and Shinichi Yamauchi

Mitsubishi Chemical Corporation, Yokkaichi Research Center, Toho 1, Yokkaichi, Mie, 510-0848 Japan

Katsuhiko Takagi

Department of Crystalline Materials Science, Graduate School of Engineering, Nagoya University, Furo-Cho, Chikusa-ku, Nagoya, 464-8603 Japan

Yoshiaki Ukai and Yushu Matsushita*

Department of Applied Chemistry, Graduate School of Engineering, Nagoya University, Furo-Cho, Chikusa-ku, Nagoya, 464-8603 Japan

Received June 29, 2000; Revised Manuscript Received October 10, 2000

ABSTRACT: The miscibility of perdeuterated isotactic polypropylene (d-PP) and ethylene−1-hexene random copolymer (EHR) blends, which were polymerized by metallocene catalyst, was investigated by small-angle neutron scattering (SANS) with changing hexene content in EHR and temperature above the melting point of d-PP. Flory−Huggins interaction parameter ($\chi_{d-PP/EHR}$) between two polymers was determined on the basis of random phase approximation (RPA). It was revealed that $\chi_{d-PP/EHR}$ decreases with increasing hexene content in EHR, which contain hexene ranging from 26 to 46 mol %, and with increasing temperature; however, the χ parameter between d-PP and atactic poly(1-hexene) was larger than that between d-PP and EHR with 46 mol % of hexane, and it increased with increasing temperature. Scattering intensities from d-PP and isotactic poly(1-hexene) blend could not been explained by RPA, being concluded that these two polymers are immiscible.

I. Introduction

Isotactic polypropylene (PP) is a widely used plastic with easy processing and excellent properties. The miscibility of PP and ethylene−α-olefin random copolymer blends has been studied intensively due to scientific interest and industrial importance. Since blending of elastomeric ethylene−α-olefin random copolymers, e.g., ethylene−propylene (EPR), ethylene−butene (EBR), ethylene−hexene (EHR), and ethylene−octene random copolymers (EOR), with PP extensively enhances the physical and mechanical properties of PP in the melt and in the solid state. The immiscible blends, where elastomeric copolymer is dispersed in PP matrix, lead to tough but high modulus materials,[1−3] while the miscible blends, which possess low glass transition temperature, lead to flexible and elastic materials.[4]

In the past decade developments of metallocene catalyst made enable to copolymerize ethylene and α-olefins covering the entire feasible composition range, and the random incorporation led to the uniformity in terms of composition independent of molecular weight. The stereoregularity of polymer is also variable through the design of the stereostructure of the ligand of the catalyst.

It has been reported that the miscibility of two different olefin random copolymers is strongly affected by the microstructure of random copolymers, such as monomer structure, chain stiffness, and energetic asymmetries.[5−8] The interactions between PP and metallocene based α-olefin random copolymers have also been studied intensively in terms of the microstructure of random polymers.[9,10] Carriere et al.[11] studied the interfacial tension (γ) between PP and ethylene−octene random copolymers in the melt, which can be related to the Flory−Huggins interaction parameter (χ) for the blend by the mean field theory,[12,13] and it was reported that γ depends on the length and content of the short branch and also reported that γ decreases with increasing octene content in random copolymer. In our previous study on the miscibility between PP and ethylene-d_4−propylene random copolymers (d-EPR) prepared from metallocene catalyst, the χ value obtained by small-angle neutron scattering (SANS) for PP and d-EPR containing 47 mol % of deuterated ethylene unit is approximately 5.0×10^{-3}, while it is smaller when ethylene content is 19 mol %.[14] Weimann and coworkers[15] reported that atactic poly(ethylene−ethylethylene) random copolymers containing from 73 to 90 wt % of ethylethylene unit is miscible in the melt from SANS experiments. Yamaguchi et al. reported that the blends of PP/EBR and PP/EHR blends, both copolymers including more than 50 mol % of α-olefin, are miscible in the melt and also reported that the random copolymer exists in the amorphous phase of PP in the solid state from viscoelastic measurements, TEM observations, and the crystallization kinetics measurements.[16−18] To our knowledge, however, it has never been studied quantitatively the thermodynamic interaction between PP and EHRs which were polymerized from metallocene catalyst. In this study, therefore, miscibility between deuterated polypropylene (d-PP) and EHRs with different hexene content polymerized from metallocene catalyst in the melt was investigated by SANS with changing temperature. The miscibility between d-PP and isotactic or atactic poly(1-hexene) was also investigated in order to evaluate the effects of stereoregularity of the *n*-butyl side group in EHR on the miscibility. Chemical structures of monomeric units of PH, EHR, and d-PP are described later.

10.1021/ma001142g CCC: $19.00
Published on Web 11/28/2000

PH: -(CH$_2$-CH)-
|
C$_4$H$_9$

EHR: -(CH$_2$-CH$_2$)$_{(1-m)}$--(CH$_2$-CH)$_m$-
|
C$_4$H$_9$

d-PP: -(CD$_2$-CD)-
|
CD$_3$

II. Experimental Section

Preparation and Characterization of Polymers. Deuterated isotactic polypropylene (d-PP) was obtained by the polymerization of perdeuterated propylene (C_3D_6) with metallocene catalyst of dimethylsilylenebis(2-methyl-4,5-benzoindenyl)zirconium dichloride. The hydrogenated PP(h-PP), which possesses almost the same degree of polymerization and molecular weight distribution as d-PP, was also prepared by polymerizing regular propylene (C_3H_6). Isotactic pentad fraction for h-PP was evaluated by ^{13}C NMR using a JEOL NMR model JNM-GSX270.

1-Hexene was copolymerized with ethylene in heptane at 70 °C under pressure of 5 atm for 1 h with metallocene catalyst of dimethylsilylenebis(2-methyl-4-phenylazrenyl)hafnium dichloride (D2M4P-Hf) under the existence of cocatalysts, triisobutylaluminum (TIBA), and triphenylcarbil tetrakis(pentafluorophenyl)borate. Four copolymers with different hexene content ranging from 26 to 46 mol % were obtained, and they have been named EHR-*m*, where *m* indicates the hexene content in mol %. Two kinds of poly(1-hexene) (PH) were also prepared by using two different catalysts: one from D2M4P-Hf which produces isotactic poly(1-hexene) and the other from bis(*n*-butyl-cyclopentadienyl)zirconium dichloride (BCp-Zr) which gives atactic poly(1-hexene); they were named i-PH and a-PH, respectively.

As-polymerized EHRs and PHs were dissolved in toluene, and then the solutions were filtered with a membrane filter in order to remove the residual of catalyst. After the filteration, the EHRs and PHs were dried up by evaporation. All parent EHRs and PHs were fractionated with a preparative GPC (Japan Analytical Industry Co., Ltd. model LC-908 with a column of JAIGEL-3H-A) from 1.0 wt % of chloroform solution. Fractionated EHR were coded EHR-*mX*, where the added letter *X* indicates fraction code; for example, EHR-26G means the G*th* fraction of the parent HER-26, which includes 26 mol % of hexene, while fractionated PHs were also named in a similar manner as fractionated EPRs, e.g., a-PH-E means E*th* fraction of a-PH.

The hexene content in the fractionated EHRs and corresponding parent EHR were measured by ^{13}C NMR so as to check the inhomogeneity of hexene content. EHRs and PHs were dissolved in *o*-dichlorobenzene with benzene-d_6 as the lock material. ^{13}C NMR spectra of EHRs were analyzed on the basis of the methods reported by Asakura.[19]

Weight-averaged molecular weight (M_w) and polydispersity (M_w/M_n) of PPs and fractionated EHRs were measured by a GPC with an online multiangle laser light scattering photometer (GPC-MALLS) at 413.2 K. Further details for measurements and data treatments were described in a previous paper.[14] From M_w values, weight-averaged degree of polymerization (N_w) were obtained by dividing M_w by averaged molar mass of the repeat unit, i.e., $M_w/42$, $M_w/48$, $M_w/(28(1-m)+84m)$, and $M_w/84$ for h-PP, d-PP, EHRs, and PHs, respectively, where *m* denotes the hexene mole fraction incorporated in random copolymers.

Densities of PPs and parent EHRs were measured by a density gradient column at 23 °C. Their specific volumes at elevated temperature, ranging from 25 to 280 °C at intervals of ca. 10 °C, were evaluated by dilatometory. The melting point (T_m) of d-PP and h-PP was determined by differential scanning calorimetry (DSC), and its heating rate was 10 °C/min.

To evaluate the polymer/solvent interaction by measuring the second virial coefficient (A_2), wide-angle light scattering (WALS) measurements were performed for fractionated EHRs dissolved in mixed solvent of hexane (C_6H_{14}) and ethyl acetate ($C_4O_2H_8$) (2:1 vol/vol). Solutions of EHR-26F dissolved in mixed solvent of deuterated hexane (C_6D_{14}) and deuterated ethyl acetate ($C_4O_2D_8$) (2:1 vol/vol) were also measured to estimate the deuteration effect of the solvent on interaction between a polymer and a solvent molecule. Measurements were performed at 20 ± 0.1 °C and with the angular range from 30° to 130° at interval of 10° using a light scattering photometer equipped with a He−Ne laser (6328 Å). The refractive index increments (d*n*/d*c*) were measured by means of a differential refractometer. Solutions with five different polymer concentrations, *c*, ranging from 1.0×10^{-5} to 5.0×10^{-5} g/mL, were prepared and filtered. M_w and A_2 were obtained from Zimm plots neglecting higher-order terms in virial expansion form; the latter was evaluated from the slope of $Kc/R(\theta)$ against *c* in the limit of zero scattering angle, where *K* is the optical constant of the system and $R(\theta)$ is the excess Rayleigh's ratio.

Small-Angle Neutron Scattering (SANS). Fractionated EHRs were weighted and dissolved in a mixed solvent of deuterated hexane (C_6D_{14}) and deuterated ethyl acetate ($C_4O_2D_8$) (hexane:ethyl acetate = 2:1 vol/vol) in order to evaluate the *z*-averaged radius of gyration in a poor solvent. These two deuterated solvents were purchased from Isotec Inc. and used without any further treatment. Three solutions with different concentrations ranging from 5 to 40 mg/mL were prepared for each EHRs, and SANS measurements were carried out using quartz cells with 1 mm in thickness.

Almost equal amounts of d-PP and h-PP were weighted and codissolved in toluene at ca. 105 °C in order to prepare a homogeneous equal volume mixture. Hot toluene solution of the mixture was poured into cold methanol, and the precipitates were filtered followed by drying under vacuum at room temperature. The homogeneous blend samples of the fractionated EHRs and d-PP were also prepared by the same way adopted for h-PP and d-PP(h-PP/d-PP(50:50)) blend; they are summarized in Table 4. The dried powders were press-molded at room temperature to form disks for SANS measurements, which possessed 20 mm diameter and 1.5 mm thickness. A 0.1 wt % sample of commercial antioxidant (IRGANOX1010 from Cyba) was added to all blend samples in order to prevent the thermal degradation during SANS measurements at elevated temperatures.

SANS experiments were carried out on the SANS-U spectrometer of the Institute for Solid State Physics, the University of Tokyo, installed in JRR-3M at Tokai. The experiments were conducted with cold neutrons whose wavelength λ was 7.0 Å with its distribution $\Delta\lambda/\lambda$ of 0.1 and sample-to-detector distances adopted were 2, 4, and 8 m. The scattering vector (**q**) is defined as $|\mathbf{q}| = 4\pi \sin(\theta)/\lambda$, where 2θ is the scattering angle. The data sets measured at different sample-to-detector distances were connected together to acquire scattering curves covering wide $|\mathbf{q}|$ range. Further details for data reduction and absolute calibration were described in our previous paper [14] and in a ref 20. SANS measurements for EHR in mixed solvents were performed at 20 ± 0.1 °C, while those for h-PP/d-PP (50:50) and d-PP/EHR blends were done at various temperatures ranging from 155 to 270 °C controlled by TEMCON using sample holders with quartz windows under vacuum. The lower temperature range was limited by the melting point of PPs.

III. SANS Data Analysis

The coherent cross section ($d\Sigma/d\Omega$) from an EHR molecule in a dilute solution can be expressed at small angle as

$$\frac{d\Sigma}{d\Omega} \propto \exp(-q^2 R_{g\langle z\rangle}{}^2/3) \quad \text{for } qR_{g\langle z\rangle} < 1 \tag{1}$$

where $R_{g\langle z\rangle}$ denotes the z-averaged radius of gyration of the polymer. The subscript $\langle z\rangle$ will be omitted for simplicity hereafter.

The coherent cross section of a blend of labeled and unlabeled polymer is given by eq 2,

$$\frac{d\Sigma}{d\Omega} = (a_D/v_D - a_H/v_H)^2 S(q) \tag{2}$$

where a_D and a_H are scattering lengths of monomers of labeled and unlabeled PP in the present case,[21] which have the specific molar volumes v_D and v_H, respectively. The structure factor $S(q)$ in eq 2 is given by eq 3 based on the random phase approximation (RPA),[22]

$$S(q)^{-1} = [v_D N_{w,D} \phi_D P_D(q^2 R_{g,D}{}^2)]^{-1} + [v_H N_{w,H}(1 - \phi_D) P_H(q^2 R_{g,H}{}^2)]^{-1} - 2\chi_{DH}/v_0 \tag{3}$$

where ϕ_D is the volume fraction of the labeled component and $R_{g,D}$, $R_{g,H}$, $N_{w,D}$, and $N_{w,H}$ denote radii of gyration and weight-averaged degree of polymerizations and molar volumes of labeled (subscript D) and unlabeled (subscript H) species, respectively, while χ_{DH} is the Flory−Huggins interaction parameter between labeled and unlabeled polymers. The reference volume v_0 is defined as

$$v_0 = (v_D v_H)^{1/2} \tag{4}$$

and $P_i(q^2 R_{gi}{}^2)$ (i = D or H) in eq 3 denotes the particle scattering factor of component i; it was assumed to be represented by the Debye function. The averaging with respect to the molar mass[23,24] was performed assuming a Shultz−Zimm distribution, and this procedure yields eq 5.

$$P_i(q^2 R_{g,i}{}^2) = \frac{2[(1 + U_i \xi_i)^{-1/U_i} + \xi_i - 1]}{(1 + U_i)\xi_i{}^2} \tag{5}$$

$$\xi_i = \frac{q^2 R_{g,i}{}^2}{1 + 2U_i} \tag{6}$$

$$U_i = \frac{N_{w,i}}{N_{n,i}} - 1 \tag{7}$$

If labeled and unlabeled species possess the same N_w and N_w/N_n, one can describe $N_{w,D} = N_{w,H}$ and hence $U_D = U_H$. Furthermore, if we assume that the statistical segment lengths of labeled and unlabeled species are the same since their specific molar volumes are very close in the melt, i.e., $v_D = v_H = v$, we can write $R_{g,H} = R_{g,D} = R_g$. When the volume fraction of two species are the same, i.e., $\phi_D = \phi_H = 0.5$, the structure factor in eq 3 can be much simplified, and it is given as

$$S(q)^{-1} = [{}^1/_4 v N w P(q^2 R_g{}^2)]^{-1} - 2\chi_{DH}/v \tag{8}$$

The structure factor for the miscible blends was given by expanding the idea of RPA. The particle scattering factor of d-PP, $P_{d-PP}(q^2 R_{g,d-PP}{}^2)$, should be obtained from D/H blend experiment, namely from eq 8, while that of EHR, $P_{EHR}(q^2 R_{g,EHR}{}^2)$, can be given by using R_g determined by dilute solution experiments in a poor solvent actually expressed in eq 1, both considering the effects of polydispersity which can be evaluated from eq 5. Consequently, the structure factor for d-PP/EHR blend is given as

$$S(q)^{-1} = [v_{d-PP} N_{w,d-PP} \phi_{d-PP} P_{d-PP}(q^2 R_{g,d-PP}{}^2)]^{-1} + [v_{EHR} N_{w,EHR}(1 - \phi_{d-PP}) P_{EHR}(q^2 R_{g,EHR}{}^2)]^{-1} - 2\chi_{d-PP/EHR}/v_0 \tag{9}$$

where $\chi_{d-PP/EHR}$ is the interaction parameter between d-PP and EHR.

IV. Results and Discussion

N_w, M_w/M_n, and the other characteristics of h-PP and d-PP are listed in Table 1. It is apparent from this table that N_w and M_w/M_n for d-PP and h-PP are almost the same. The isotactic pentad fraction [mmmm] and inversion caused by hydrogen elimination of h-PP were determined by ^{13}C NMR,[25,26] though [mmmm] of d-PP could not be evaluated due to the coupling of deuterium and carbon. The melting point of h-PP and d-PP determined by DSC was 150 and 147 °C, respectively. Since N_w and M_w/M_n of d-PP and h-PP are almost the same, it is reasonable to set $N_{w,d-PP} = N_{w,h-PP} = (N_{w,d-PP} N_{w,h-PP})^{1/2} = 1076$ and $(M_w/M_n)_{d-PP} = (M_w/M_n)_{h-PP} = 1.8$ on analyzing SANS data with using eqs 5−8.

The background corrected coherent cross section for d-PP/h-PP(50/50) at 164.5 °C is plotted against q in Figure 1. The solid line in Figure 1 is a best-fitted one drawn by the nonlinear least-squares method by varying R_g as a parameter in particle scattering factor (P) in eq 8 assuming the Debye function and also assuming that χ_{DH} is negligibly small. The R_g value estimated from this method was 88.0 Å. The R_g's thus obtained at various temperatures are plotted in Figure 2. It is evident that they are almost constant within the temperature (t) range studied in this work, i.e., 164.5 °C ≤ t ≤ 255.9 °C. The constant value of R_g, 88.0 Å, was used on analyzing SANS data from d-PP/EHR and d-PP/PH blends.

Hexene content, molecular weight distribution (M_w/M_n), and density of parent EHRs and PHs are listed in Table 2. It was confirmed that stereoregularity of i-PH, polymerized from D2M4P-Hf, was isotactic, while PH from BCp-Zr was atactic since the isotactic triad [mm] of i-PH was 98 mol %, while a-PH contained 3.8 mol % of 2−1 inversion, though any other irregularities ascribed to the β hydrogen elimination were not detected. M_w obtained by GPC-MALLS and corresponding N_w for fractionated EHRs and PHs are summarized in Table 3. The hexene contents of the fractionated EHRs agree well with those of their parent EHRs within the experimental errors. Since M_w values determined from GPC-MALLS are in good agreement with those obtained from WALS, the former values were used for data analysis. Densities at room temperature and their temperature dependence of the fractionated EHRs were assumed to be identical to the corresponding parent EHRs. In Figure 3 Guiner plots of coherent cross sections from EHR-40E solutions with different concentrations are presented as an example. From the initial slope of these plots in the low q range ($qR_g < 1$), apparent radii of gyration at each concentration can be evaluated according to eq 1. From the extrapolation of

Table 1. Molecular Characteristics of PP

sample	M_w (g/mol)	M_w/M_n[a]	N_w[b]	[mmmm][c] (mol %)	2,1 inversion[c] (mol %)	1,3 inversion[c] (mol %)	density (g/cm^3)	T_m (°C)
h-PP	45 800	1.78	1090	96	0.4	0	0.904_2	$150._0$
d-PP	51 000	1.80	1063				1.040_6	$146._5$

[a] Determined by GPC calibrated by commercially distributed standard polystyrene. [b] Weight-averaged degree of polymerization calculated from $M_w/42$ and $M_w/48$ for h-PP and d-PP, respectively. [c] Isotactic pentad fraction [mmmm] and regioirregularity (inversion) determined by ^{13}C NMR.

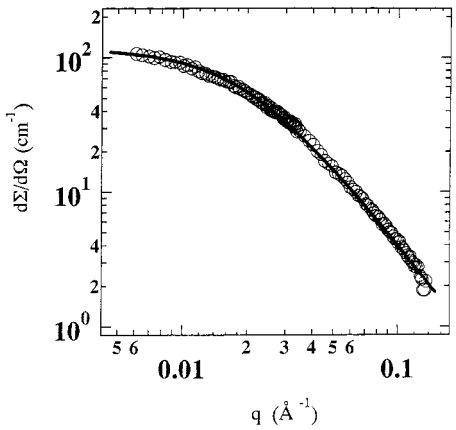

Figure 1. Background corrected coherent cross section of h-PP/d-PP (50:50) blend at 164.5 °C plotted against q. Solid line indicates the calculated one for $\chi_{HD} = 0$.

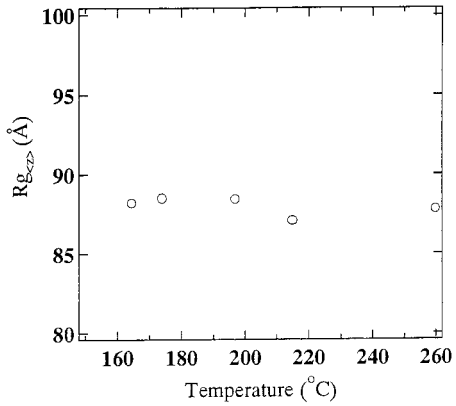

Figure 2. z-averaged radii of gyration ($R_{g\langle z\rangle}$) of PP plotted against temperature.

Table 2. Molecular Characteristics of Parent EHR and PH

sample	hexene cont[c] (mol %)	M_w/M_n[d]	density (g/cm^3)	comments
EHR-26	26	1.89	0.853_1	
EHR-35	35	1.71	0.851_5	
EHR-40	40	1.88	0.853_6	
EHR-46	46	2.03	0.853_4	
a-PH[a]	100	1.70	0.849_2	2−1 inversion: 3.8 mol %[c]
i-PH[b]	100	2.06	0.852_1	[mm]: 98 mol %[c]

[a] Atactic poly(1-hexene) polymerized from BCp-Zr. [b] Isotactic poly(1-hexene) polymerized from D2M4P-Hf. [c] Determined by ^{13}C NMR. [d] Apparent value estimated from GPC calibrated with standard polystyrene.

R_g thus obtained to zero concentration as shown in Figure 4, R_g of this sample can be estimated to be 46.0 Å. R_g data for all the fractionated EHRs are listed in Table 3.[27,28]

A_2 values of all the EHRs in mixed solvent of regular hexane and regular ethyl acrylate (2:1 vol/vol) estimated from light scattering measurements are almost the same irrespective of hexene content and are about 1.0 $\times$ 10^{-3} mol mL/g^2, while that of EHR26-F in the deuterated mixed solvent is also 1.0 $\times$ 10^{-3} mol mL/g^2. This fact implies that there is no essential deuteration effect on evaluating chain dimension of EHRs in the present mixed solvent. Although the mixed solvent is not a Θ solvent for any EHRs, it is reasonably poor because A_2 values are reasonably small. Thus, we have a good reason to assume that R_g's of EHRs obtained in the mixed solvent would be fairly close to their unperturbed dimensions; therefore, we used them on analyzing SANS coherent scattering profiles.

In Figures 5 the background corrected coherent cross sections from d-PP/EHR blends at different temperatures are plotted against q, while that for the d-PP/a-PH-E (53:47) blend is presented in Figure 6. Comparing parts a−d of Figure 5, it was found that coherent cross sections from d-PP/EHR-26G (55:45) in Figure 5a at low q decreases with increasing temperature, while those from the blends that include EHRs with higher hexene content, i.e., EHR35 in Figure 5b, EHR40 in Figure 5c, and EHR46 in Figure 5d, vary a little with temperature or variation is undetectable. Alternatively, those from d-PP/a-PH-E (53:47) in Figure 6 increase with increasing temperature. It means the sign of temperature dependence of $\chi_{d-PP/EHR}$ turns over with varying hexene content in EHR.

To evaluate $\chi_{d-PP/EHR}$ for the blends, SANS coherent cross sections were fitted to eq 9 via eq 2 assigning χ as a fitting parameter, introducing 88.0 Å for R_g of d-PP, R_g's of EHR, and $N_{w,d-PP}$, $N_{w,EHR}$, and ϕ_{EHR} values listed in Table 3 and also introducing v_{d-PP} and v_{EHR} values estimated from the dilatometric study. Three data sets at certain temperatures were picked up from data in Figures 5a,b and 6, and curve fittings to the calculated intensities are presented in Figure 7, parts a (d-PP/EHR-26G (55:45)), b (d-PP/EHR-35F (53:47)), and c (d-PP/a-PH-E (53:47)). All the data sets were fitted well covering the entire q range, and best-fitted results are expressed by bold solid lines. The interaction parameter at thermodynamic stability limit (χ_s), that is, χ at spinodal point of the blend, is defined as eq 10.[29]

$$\chi_s = \frac{v_0}{2}\left[\frac{1}{v_{EHR}N_{w,EHR}\phi_{EHR}} + \frac{1}{v_{d-PP}N_{w,d-PP}(1-\phi_{EHR})}\right] \quad (10)$$

The calculated coherent cross section using χ_s corresponding to this limit is also drawn in Figure 7 as dashed dotted lines. From these figures it was confirmed that all χ values evaluated are sufficiently smaller than χ_s, their values and are shown in the captions of Figure 7. In Figure 8 background corrected coherent cross sections for d-PP/i-PH-A (60:40) at different temperatures are plotted against q, where dΣ/dΩ strongly depends on q. In the low q range (q < 0.01) dΣ/dΩ decays as q^{-4}, and in the higher q range (q > 0.01) it depends on q^{-2}. These q dependences cannot be explained by

Table 3. Molecular Characteristics of Fractionated Random Copolymers

sample	hexene cont (mol %)	M_w (g/mol)	M_w/M_n	N_w[a]	$R_{g\langle z\rangle}$[b] (Å)	$R_{g\langle z\rangle}^2/M_w$ (Å^2 mol g^{-1})
EHR-26G	26	9 960	1.25	234	36.9	0.137
EHR-26F	26	16 300	1.22	383	44.8	0.123
EHR-35F	35	12 900	1.20	271	36.2	0.102
EHR-35G	35	9 050	1.19	190	29.3	0.095
EHR-40E	40	21 900	1.07	435	46.0	0.097
EHR-40F	40	15 900	1.16	315	34.5	0.075
EHR-46D	46	45 980	1.16	856	70.0	0.107
EHR-46E	46	31 200	1.25	580	50.1	0.080
a-PH-E	100	10 100	1.20	120	26.0	0.067
i-PH-A	100	77 700	1.40	925		

[a] Estimated from M_w. Relationships between M_w and N_w are written in the text. [b] z-averaged radius of gyration determined by SANS.

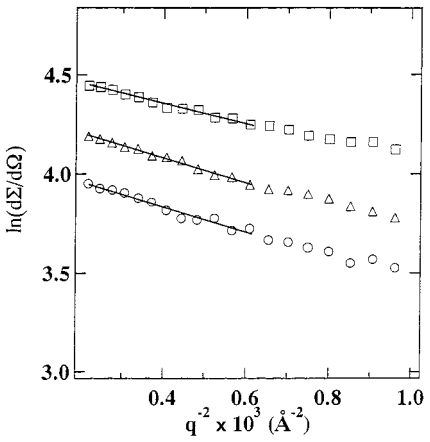

Figure 3. Guiner plots of coherent intensities for the solutions of EHR-40E at 20 °C. Concentrations of solutions are 12.4 mg/mL (circles), 18.6 mg/mL (triangles), and 37.0 mg/mL (squares).

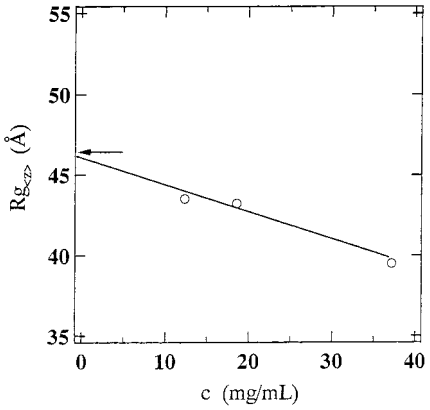

Figure 4. Polymer concentration (c) dependence of z-averaged radius of gyration determined by Guiner plots for EHR-40E solutions. An arrow indicates the extrapolated R_g value of 46.0 Å.

RPA for miscible blends. Accordingly, their Ornstein−Zernike plots give the negative intercept at q equals 0. Considering these results it would be concluded that the blend of d-PP and i-PH is immiscible within the temperature range adopted in this study.[41] This was supported by the phase contrast optical microscope observation for the blends quenched from the melt. χ estimated for this blend system is larger than χ_s, i.e., 2.1×10^{-3} covering the entire temperature range studied. It is not possible to conclude the effect of stereoregularity of PH, i.e., atactic and isotactic sequences, on the miscibility to d-PP from these results only.

In Figure 9 $\chi_{d-PP/EHR}$ and $\chi_{d-PP/a-PH}$ are plotted against the inverse of the absolute temperature. In general, the temperature dependence of experimentally obtained χ is known to be expressed by the following form:

$$\chi_{exp} = A + B/T \tag{11}$$

where T is the absolute temperature and A and B are constants. For the present blends it is evident that the A value is positive and decreases with increasing hexene content in EHR ranging from 26 to 46 mol %; however, the blend with atactic polyhexene possesses a larger χ value. B for d-PP/EHR-26 is positive and about 2.0 K and suddenly drops and becomes almost zero with increasing hexene content in EHRs, whereas d-PP/a-PH-E (53:47) possesses negative B, which is −1.7 K.

Krishnamoorti[30] and Reichart et al.[31] have reported the same types of thermodynamic interaction as observed for the d-PP/a-PH blend in which the χ decreases with increasing temperature for hhPP/PIB, atactic PP/PEP, and atactic PP/PEB, where hhPP, PIB, PEP, and PEB denote head-to-head polypropylene, polyisobutylene, poly(ethylene−propylene), and poly(ethylbutadiene), respectively. The PIB/hhPP blend possesses negative χ value, which increases with temperature resulting in phase separation.[30] Such behavior has been commonly observed for the blend system where the miscibility is driven by some specific association between the components.[32] Recently, Freed et al.[33−35] developed the analytical expression for free energy of homogeneous binary blend of homopolymer based on the lattice cluster theory (LCT) and succeeded in explaining the LCST phase diagram observed for PIB and hhPP using the exchange energy (ϵ) as an adjustable parameter.[35,36] In their theory the influence of monomer topology and the effect of the nonrandom mixing are considered. It was concluded that the LCST phase diagram is ascribed to a competition between the stabilizing influence of negative ϵ and the entropic destabilization from the structural disparity. Applying the LCT to the experimentally obtained $\chi_{d-PP/a-PH}$ for d-PP/a-PH-E (53:47), eq 12 can be given using eq 11 in ref 35 regardless of the fraction of regioirregularity of a-PH and assuming the volume fraction of d-PP equals 0.5.

$$\chi_{d-PP/a-PH} = \sqrt{18}\left\{\frac{1}{6^2}\left(\frac{1}{6}\right)^2 + \left(\frac{\epsilon}{kT}\right)\left[2 - \frac{p_{d-PP}}{12} - \frac{p_{a-PH}}{12}\right] - \left(\frac{\epsilon}{kT}\right)^2\left[1 + \frac{r_{d-PP}}{4} + \frac{r_{a-PH}}{4}\right]\right\} \tag{12}$$

where r_{d-PP}, r_{a-PH}, p_{d-PP}, and p_{a-PH} are the geometrical coefficients,[35,36] which are introduced to characterize the monomer molecular structure in LCT, and are set to be $^4/_3$, $^7/_6$, $^4/_3$, and $^8/_6$, respectively, and k is the Boltzmann constant. The exchange energy ϵ is defined as $\epsilon =$

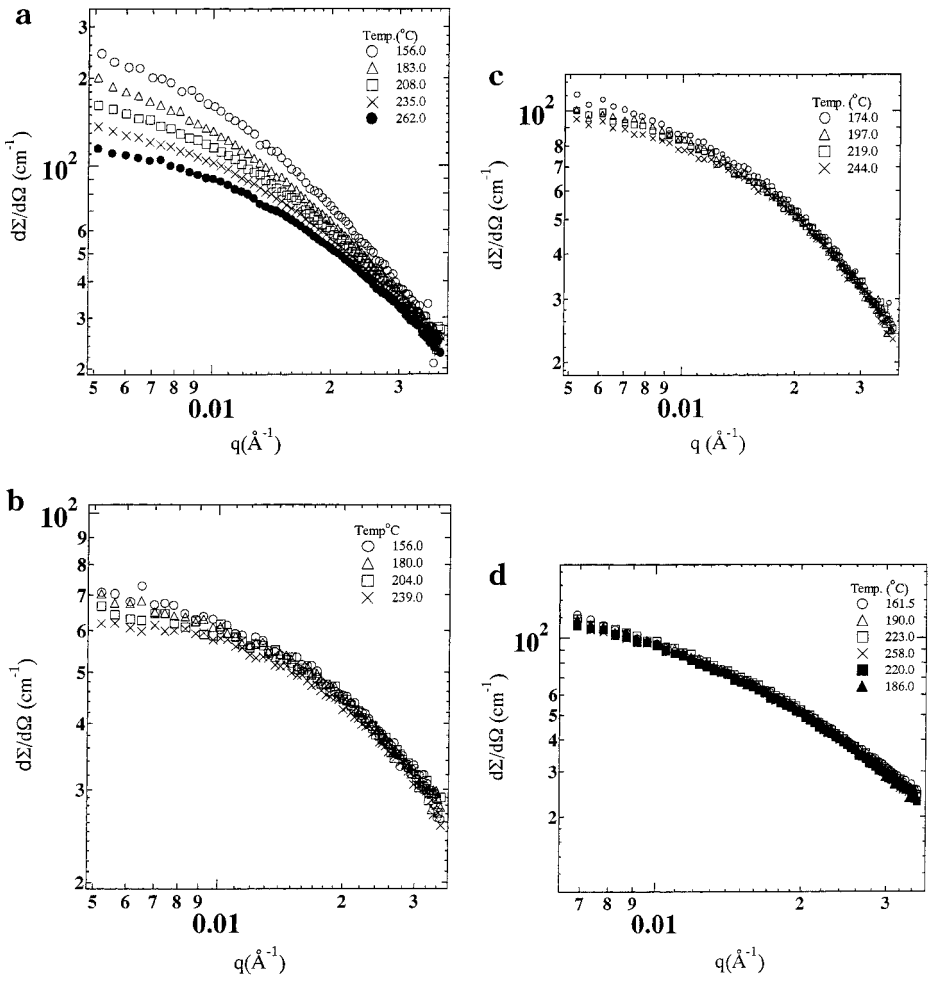

Figure 5. Background corrected SANS coherent cross sections for several d-PP/HER blends at various temperature: (a) d-PP/EHR-26G (55:45), (b) d-PP/EHR-35F (53:47), (c) d-PP/EHR-40G(54:46), and (d) d-PP/EHR-46D (52:48).

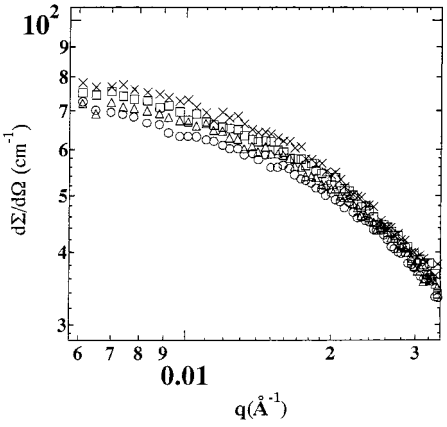

Figure 6. Background corrected SANS coherent cross sections for blend of d-PP/a-PH-E (53:47) at different temperatures: (○) 164.0, (△) 196.0, (□) 222.0, and (×) 250.0 °C.

$\epsilon_{d-PP/d-PP} + \epsilon_{a-PH/a-PH} - 2\epsilon_{PP/a-PH}$, where $\epsilon_{\alpha/\beta}$ is the van der Waals energy between neighboring united atom groups of species α and β. χ's were calculated for two ϵ's and are presented as a function of inverse of the absolute temperature in Figure 10. The solid and dotted lines are χ for ϵ of 0 and $-0.025K$, respectively. The absolute ϵ value for the blend is considered to be small and is on the order of $10^{-2}K$. The negative sign of B for d-PP/a-PH blend may be caused by the same reason as for the blend of PIB/hhPP,[35] that is, energetic origin ascribed to negative ϵ.

The variation of $\chi_{d-PP/EHR}$ at 200 °C, which are estimated from Figure 9 with hexene content in EHR, is presented in Figure 11 and summarized in Table 4. The temperature of 200 °C was chosen voluntarily as one of the intermediate temperatures within the range adopted in this study, i.e., 155 °C ≤ t ≤ 270 °C. Within the composition range of 0.26 ≤ m ≤ 0.46, $\chi_{d-PP/EHR}$ decreases monotonically with hexene content in EHR, while a-PH possesses an apparently higher value than expected. The decrease of $\chi_{d-PP/EHR}$ with increasing hexene content is qualitatively consistent with the results by other researchers.[16,18] Recently, the comonomer composition dependence of χ for the blend of a homopolymer A and a random copolymer C_mD_{1-m} was also analyzed by LCT;[37] therefore, the method was applied to the present case, where components A, C, and D correspond to d-PP, a-PH, and PE, respectively. $\chi_{d-PP/EHR}$ can be expressed as eq 13 according to eq 20 in ref 37,[38]

$$\chi_{d-PP/EHR} = \sqrt{12m+6}\left\{\frac{1}{6^2}\left(\frac{m+2}{12m+6}\right)^2 + \frac{6}{12m+6} \times \left[3m\chi^{LCT}_{d-PP/a-PH} + (1-m)\chi^{LCT}_{d-PP/PE} - \frac{18}{12m+6}m(1-m)\chi^{LCT}_{a-PH/PE}\right]\right\} \quad (13)$$

where m is the mole fraction of hexene in EHR and $\chi^{LCT}_{i/j}$ expresses the *enthalpic* part of interaction between pure components i and j.[38] Since $\chi_{d-PP/EHR}$ actu-

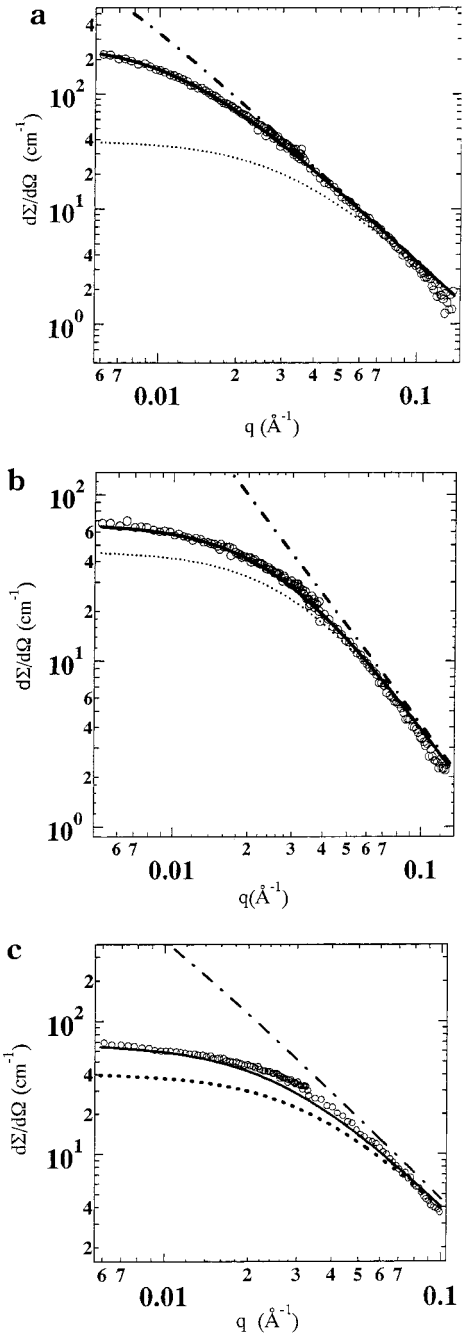

Figure 7. Background corrected SANS coherent cross sections for three blends at certain temperatures plotted against q: (a) d-PP/EHR-26G (55:45) blend at 156.0 °C, (b) d-PP/EHR-35F (53:47) at 156.0 °C, and (c) d-PP/a-PH-E (53:47) at 164.0 °C. Dotted lines and dashed dotted lines indicate calculated dΣ/dΩ for $\chi = 0$ and $\chi = \chi_s$, while solid lines indicate the best fitted dΣ/dΩ, where χ adopted are 0.048, 0.0016, and 0.003 for d-PP/EHR-26G (55:45), d-PP/EHR-35F (53:47), and d-PP/a-PH-E (53:47), respectively.

ally becomes $\chi^{LCT}_{d-PP/a-PH}$ when m equals unity in eq 13, the $\chi^{LCT}_{d-PP/a-PH}$ at 200 °C can be estimated to be 3.0×10^{-5} using 3.3×10^{-3} for $\chi_{d-PP/EHR}$ in Table 4. Note that the former value is negligibly small compared to the latter. This means the dominant contribution to $\chi_{d-PP/EHR}$ is the entropic term, the first term in eq 13. Using $\chi^{LCT}_{d-PP/a-PH}$ thus estimated at m equal to 1 as a boundary condition, $\chi_{d-PP/EHR}$ was fitted to eq 13 regarding $\chi^{LCT}_{d-PP/PE}$ and $\chi^{LCT}_{a-PH/PE}$ as two adjustable parameters, and a solid line was given; two parameters thus expediently estimated are 6.5×10^{-3} and 14.5×10^{-3},

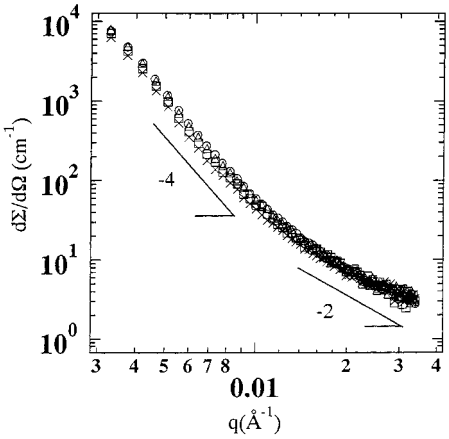

Figure 8. Background corrected SANS intensity for d-PP/i-PH-A (60:40) at various temperatures: (○) 164.9, (△) 159.9, (□) 201.9, and (×) 237.4 °C. Solid line indicates q^{-4}.

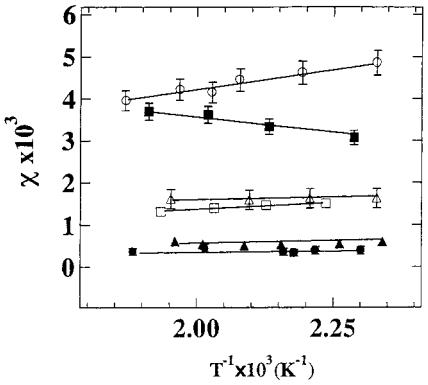

Figure 9. $\chi_{d-PP/EHR}$ for d-PP/EHR and d-PP/a-PH blends plotted against inverse of the absolute temperature: (○) d-PP/EHR-26G (55:45), (△) d-PP/EHR-35F (52:48), (□) d-PP/EHR-40E (54:46), (●) d-PP/EHR-46D (52:48), (▲) d-PP/EHR-46E (62:38), (■) d-PP/a-PH-E (53:47). Error bars are estimated by considering uncertainties came from both molecular weight determination and data reduction procedure in analyzing SANS intensities according to Balsara et al.[29]

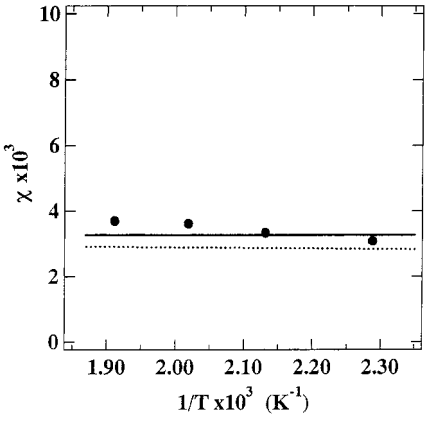

Figure 10. χ for the blend of d-PP/a-PH-E (53:47) obtained by SANS (black circles) and the χ calculated based on the lattice cluster theory plotted against inverse of absolute temperature. Solid line and dotted line correspond to χ for exchange energy (ϵ) of 0 and $-0.025K$, respectively.

respectively, both being meaningfully larger than $\chi^{LCT}_{d-PP/a-PH}$. The convex form of $\chi_{d-PP/EHR}$ in terms of m is explained by the contribution from the fourth term including $m(m-1)\chi^{LCT}_{a-PH/PE}$ in eq 13, which is actually effective as the results of the *repulsion* between ethylene and hexene units.[39,40] Thus, it is easy to understand the

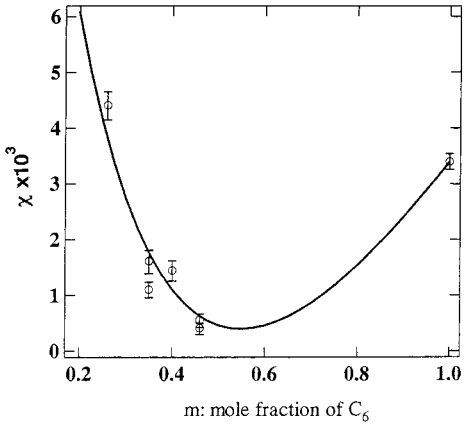

Figure 11. $\chi_{d-PP/EHR}$ for d-PP/EHR blends and d-PP/a-PH blend at 200 °C plotted against hexene content. The solid line is obtained from nonlinear least regression to eq 13 using $\chi^{LCT}_{d-PP/a-PH} = 3.0 \times 10^{-5}$ and two adjustable parameters of $\chi^{LCT}_{d-PP/PE}$ and $\chi^{LCT}_{a-PH/PE}$. Error bars are associated with those estimated in Figure 9.

Table 4. Miscibility Data for d-PP/HER and d-PP/PH Blends

blend code	vol fract of EHR[a] (vol %)	$\chi_s \times 10^{3b}$	$\chi_s \times 10^{3c}$	$d\chi/d(1/T)$ (K)
d-PP/EHR-26G(55:45)	45.3	5.5	4.4 ± 0.25	2.0
d-PP/EHR-35F(52:48)	47.2	4.8	1.6 ± 0.21	0.1
d-PP/EHR-35G(54:46)	46.0	6.3	1.1 ± 0.14	0.2
d-PP/EHR-40E(54:46)	45.9	3.4	1.5 ± 0.18	0.3
d-PP/EHR-46D(52:48)	47.7	2.1	0.4 ± 0.10	0
d-PP/EHR-46E(62:38)	38.1	2.8	0.5 ± 0.12	0
d-PP/a-PH-E(53:47)	46.7	7.3	3.3 ± 0.14	−1.7
d-PP/i-PH-A(60:40)	40.0	2.1	*d*	*d*

[a] Volume fraction of EHR at room temperature. [b] χ_s is χ at spinodal point determined by eq 10 at 200 °C. [c] χ estimated from SANS at 200 °C. [d] Not obtained because of phase separation.

thermodynamic interaction for d-PP/EHR blends by separating into two parts, i.e., entropic and enthalpic terms, by use of LCT.

V. Summary

The miscibility of d-PP and EHR was investigated by SANS with changing hexene content in EHR. The Flory−Huggins interaction parameter ($\chi_{d-PP/EHR}$) between two polymers was determined on the basis of the random phase approximation. It was revealed that $\chi_{d-PP/EHR}$ decreases with increasing hexene content in EHR up to 46 mol %, and with increasing temperature; however, the $\chi_{d-PP/a-PH}$ is larger than expected and decreased with increasing temperature. These behaviors were explained by LCT considering contact energy among component polymers.

Acknowledgment. We are grateful to Dr. H. Nagao at The Institute for Solid State Physics, The University of Tokyo, for his helpful discussion concerning the error estimation of SANS-U data.

References and Notes

(1) D'Orazio, L.; Mancarella, C.; Martuscelli, E.; Cecchin, G.; Corrieri, R. *Polymer* **1999**, *40*, 2745.
(2) Starke, J. U.; Michler, G. H.; Grellmann, W.; Seidler, S.; Gahleitner, M.; Fiebig, J.; Nezbedova, E. *Polymer* **1998**, *39*, 75.
(3) Jiang, W.; Liu, C. H.; Wang, Z. G.; An, L, J.; Jiang, B. Z.; Wang, X. H.; Zhang, H. X. *Polymer* **1998**, *39*, 3285.
(4) Otsuka, N.; Ying, Y.; Saito, H.; Inoue, T.; Takemura, Y. *Polymer* **1998**, *39*, 1533.
(5) Krishnamoorti, R.; Graessley, W. W.; Balsara, N. P.; Lohse, D. J. *Macromolecules* **1994**, *27*, 3037.
(6) Graessely, W. W.; Krishnamoorti, R.; Balsara, N. P.; Butera, A. *Macromolecules* **1994**, *27*, 3896.
(7) Schweizer, K. S. *Macromolecules* **1993**, *26*, 6050.
(8) Fredrickson, G. H.; Liu, A. J.; Bate, F. S. *Macromolecules* **1994**, *27*, 2503.
(9) Thomann, Y.; Suhm, J.; Thomann, R.; Bar, G.; Maier, R. D.; Mulhaupt, R. *Macromolecules* **1998**, *31*, 5441.
(10) Chen, C. Y.; Yunus, W. Md. Z. W.; Chiu, H. W.; Kyu, T. *Polymer* **1997**, *38*, 4433.
(11) Carriere, C. J.; Silvis, H. C. *J. Appl. Polym. Sci.* **1997**, *66*, 1175.
(12) Helfand, E.; Bhattacharjee, S. M.; Fredrickson, G. H. *J. Chem. Phys.* **1989**, *91*, 7200.
(13) Tang, H.; Freed, K. F. *J. Chem. Phys.* **1991**, *94*, 6307.
(14) Seki, M.; Nakano, H.; Yamauchi, S.; Suzuki, J.; Matsushita, Y. *Macromolecules* **1999**, *32*, 3227.
(15) Weimann, P. A.; Johns, T. D.; Hillmyer, M. A.; Bates, F. S.; Londono, J. D.; Melnichenko, Y.; Wignall, G. D.; Almdal, K. *Macromolecules* **1997**, *30*, 3560.
(16) Yamaguchi, M.; Miyata, H.; Nitta, K. *J. Appl. Polym. Sci.* **1996**, *62*, 87.
(17) Yamaguchi, M.; Miyata, H.; Nitta, K. *J. Polym. Sci., Polym. Phys. Ed.* **1997**, *35*, 953.
(18) Yamaguchi, M.; Miyata, H. *Macromolecules* **1999**, *32*, 5911.
(19) Asakura, T.; Demura, M.; Nishiyama, Y. *Macromolecules* **1991**, *24*, 2334.
(20) Ito, Y.; Imai, M.; Takahashi, S. *Physica B* **1995**, *213&214*, 889.
(21) Ulmann, R. *Annu. Rev. Mater. Sci.* **1980**, *10*, 261.
(22) de Gennes, P. G. *Scaling Concepts in Polymer Physics*; Cornell University Press: Ithaca, NY, 1979.
(23) Zirkel, A.; Urban, V.; Richter, D.; Fetters, L. J.; Huang, J. S.; Kampmann, R.; Hadjichristidis, N. *Macromolecules* **1992**, *25*, 6148.
(24) Glatter, O.; Kratky, O. *Small-angle X-ray Scattering*; Academic Press: New York, 1982.
(25) Cheng, H. N. *Macromolecules* **1984**, *17*, 1950.
(26) Ray, G. J.; Johnson, P. E.; Knox, J. R. *Macromolecules* **1977**, *10*, 773.
(27) Reichert, G. C.; Graessley, W. W.; Register, R. A. *Macromolecules* **1998**, *31*, 7886.
(28) Zirkel, A.; Urban, V.; Richter, D.; Fetters, L. J.; Huang, J. S.; Kampmann, R.; Hadjichristidis, N. *Macromolecules* **1992**, *25*, 6148.
(29) Balsara, N. P.; Fetters, L. J.; Hadjichristidis, N.; Lohse, D. J.; Han. C. C.; Graessley, W. W.; Krishnamoorti, R. *Macromolecules* **1992**, *25*, 6137.
(30) Krishnamoorti, R.; Graessley, W. W.; Fetters, L. J.; Garner, R. T.; Lohse, D. J. *Macromolecules* **1995**, *28*, 1252.
(31) Reichart, C. G.; Gaessley, W. W.; Resister, R. A.; Krishnamoorti, R.; Lohse, D. J. *Macromolecules* **1997**, *30*, 3036.
(32) Paul, D. R.; Barlow, J. W.; Keskkula, H. *Encycropedia of Polymer Science and Engineering*, 2nd ed.; Wiley: New York, 1988.
(33) Freed, K. F.; Bawendi, M. G. *J. Phys. Chem.* **1989**, *93*, 2194.
(34) Dudowicz, J.; Freed, M. S.; Freed, K. F. *Macromolecules* **1991**, *24*, 5096.
(35) Freed, K. F.; Dudowicz, J. *Macromolecules* **1998**, *31*, 6681.
(36) The monomer occupancy indices for d-PP and a-PH is $s_{d-PP} = 3$ and $s_{a-PH} = 6$, respectively. The geometrical coefficients for PP and a-PH were set to $r_{PP} = {}^4/_3$, $r_{a-PH} = {}^7/_6$, $p_{PP} = {}^4/_3$, and $p_{a-PH} = {}^8/_6$, respectively. The Flory parameter (z) was chosen to be 6.
(37) Dudowicz, J.; Freed, K. F. *Macromolecules* **2000**, *33*, 3467.
(38) $\chi^{LCT}_{i/j}$ is defined as $(z/2)(\epsilon_{ii} + \epsilon_{jj} - 2\epsilon_{ij})/kT$ where ϵ_{ij} is the monomer averaged nearest-neighbor van der Waals attractive energy between united atom groups of species *i* and *j*. s_1, s_2, r_1, and r_2, which is defined by eqs 16, 10, and 11 in ref 37, are 3, $4m + 2$, ${}^4/_3$, and $(5m + 2)/(4m + 2)$, in which *m* is the mole fraction of hexene in EHR.
(39) Kambour, R. P.; Bendler, J. T.; Bopp, P. C. *Macromolecules* **1983**, *16*, 753.
(40) Brinke, G. T.; Karasz, F. E.; Macknight, W. J. *Macromolecules* **1983**, *16*, 1827.
(41) Alamo, R. G.; Graessley, W. W.; Krishnamoorti, R.; Lohse, D. J.; Londono, D. J.; Mandelkern, L.; Stehling, F. C.; Wignall, G. D. *Macromolecules* **1997**, *30*, 561.

MA001142G